PAPER

CrossMark
click for updates

Newport Green, a fluorescent sensor of weakly bound cellular Zn^{2+}: competition with proteome for Zn^{2+}†

Mohammad Rezaul Karim and David H. Petering*

Newport Green (NPG) is a recognized sensor of cellular Zn^{2+} that displays fluorescence enhancement upon binding to Zn^{2+}. Because of its modest affinity for Zn^{2+}, the extent of its capacity to bind cellular Zn^{2+} is unclear. The present study investigated the range of reactivity of NPG_{ESTER} with cells, isolated (Zn)-proteome, and model Zn-proteins. The sensor accumulated in pig kidney LLC-PK$_1$ cells and was slowly (>40 min) hydrolyzed to the fluorescent, acid form, NPG_{ACID}. The powerful, cell permeant Zn^{2+} chelator, N,N,N',N'-tetrakis(2-pyridylmethyl)-ethane-1,2-diamine (TPEN) failed to quench the growing fluorescence emission, indicating that $Zn–NPG_{ACID}$ had not formed and $NPG–Zn$-protein adduct species probably were not present. Furthermore, NPG_{ACID} did not bind to Zn-carbonic anhydrase or Zn-alcohol dehydrogenase, two proteins that form adducts with some other sensors. Strikingly, most of the NPG_{ACID} that had been converted from NPG_{ESTER} was detected in the extracellular medium not the cells. As a result, after cells were incubated with NPG_{ESTER} and then Zn-pyrithione to raise the internal concentration of mobile Zn^{2+}, $Zn–NPG_{ACID}$ was only observed in the external medium. Residual cellular NPG_{ACID} was unable to bind extra intracellular Zn^{2+} delivered by pyrithione. Proteome isolated from the sonicated cell supernatant was also unreactive with NPG_{ACID}. Titration of proteome or glutathione with Zn^{2+} in the presence of NPG_{ACID} revealed that NPG_{ACID} only weakly competes for mobile Zn^{2+} in the presence of these cellular components. In addition, when proteomic Zn^{2+} was released by a nitric oxide donor or N-ethyl-maleimide, little Zn^{2+} was detected by NPG_{ACID}. However, exposure to nitric oxide independently enhanced the fluorescence properties of NPG_{ACID}. Thus, the biochemical properties of NPG related to cellular Zn^{2+} chelation deepen the question of how it functions as a Zn^{2+} sensor.

Introduction

A number of fluorescent biosensors have been synthesized during the past decade with the aim to detect and measure basal and elevated intracellular concentrations of metals.[1–3] Such metallic species are variously described as labile, weakly bound, or accessible metal–ligand complexes, or free metal ions.[4] Starting with a global view of intracellular metal ion (M) distribution among proteins and other ligands such as glutathione (L),

$$\sum M - Ligand_i \rightleftharpoons \sum Ligand_i + M \qquad (1)$$
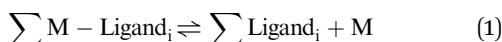
the sensor (S) may react with M to form a distinct fluorescent species, depending on its conditional stability constant for M,‡

Department of Chemistry and Biochemistry, University of Wisconsin-Milwaukee, Milwaukee, WI 53201, USA. E-mail: petering@uwm.edu; Fax: +1 414-229-5530

† Electronic supplementary information (ESI) available. See DOI: 10.1039/c5mt00167f
‡ Abbreviations: AAS, flame atomic absorption spectrophotometry; CCRF-CEM, human lymphocytic leukemia cells; DEA-NO, diethylamine NONOate; DPBS, Dulbecco's phosphate buffered saline; DTNB, 5,5-dithiobis-2-nitrobenzonic acid; LLC-PK$_1$ pig kidney tubule cells; NPG, Newport Green; NPG$_A$, NPG acid form; NPG$_E$, NPG ester form; S, Sensor; TPEN, N,N,N',N'-tetrakis(2-pyridylmethyl)ethane-1,2-diamine.

$$M + S \rightleftharpoons M-S \; (K_{stability\,constant}) \qquad (2)$$
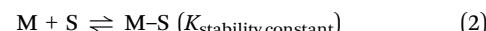
For this reaction to be quantitatively significant, the stability constant for M–S must lie within the range of concentrations of M in eqn (1). In addition, the intracellular concentration of S must be small in comparison with M, such that its presence does not perturb the equilibria embodied in reaction (1). If the stability constant of M–S or the concentration of S is too large, the sensor might significantly disturb the intracellular distribution of bound metal ion. Indeed, the sensor might react directly with M–Ligand species by ligand substitution:[5]

$$\sum M - Ligand_i + S \rightleftharpoons \sum Ligand_i + M - S \qquad (3)$$
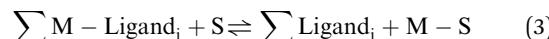
In either case, the resultant intracellular fluorescence signal of M–S would not reflect the native "free" or available metal concentration.

Sensors with a wide range of stability constants have been synthesized in order to detect metal ions linked with cellular M–Ligand complexes of different affinities for M.[1,3,6] At the lower end of this spectrum of fluorophores is Newport Green, dipotassium salt (NPG$_A$), having a stability constant of 10^5–10^6 (Fig. 1).[1,5] It is able
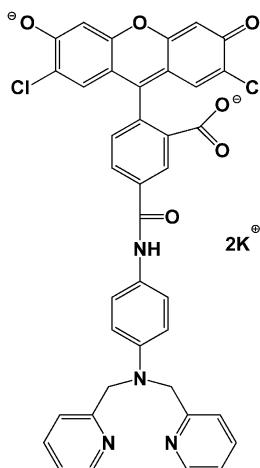
Fig. 1 Chemical structure of Newport Green, dipotassium salt (NPG$_A$).

to detect Zn^{2+} in the micromolar range through an increase in its fluorescence emission at 530 nm.[6]

A number of papers have reported the use of NPG to image cells for labile Zn^{2+}.[7–14] The total concentration of Zn^{2+} in mammalian cells is thought to fall in the 100–500 μM range.[15,16] In contrast, that of free or labile Zn^{2+} has been estimated between pM to nM.[15–18] Evidently, NPG cannot image free Zn^{2+} ion in native systems because its stability constant for Zn^{2+} is too small. Thus, it must either interact with a significant fraction of cellular Zn^{2+} that has been mobilized from its tightly bound forms, or function like the sensors TSQ and Zinquin (ZQ) to form adduct species as in reaction (4):[5,19,20]

$$NPG + \sum Zn\text{-protein}_i \rightleftharpoons \sum NPG - Zn\text{-protein}_i \quad (4)$$
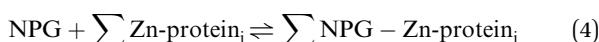
The present experiments were undertaken to understand better how NPG behaves in biological systems as a Zn^{2+} sensor.

Materials and methods

Chemicals and reagents

Newport Green, DCF diacetate (NPG$_E$) and Newport Green dipotassium salt (NPG$_A$) were purchased from Invitrogen. Newport Green was dissolved in DMSO and stored in the dark at −20 °C. All the other chemicals and reagents were purchased from either Fisher Scientific or Sigma-Aldrich at the highest grade available.

Cell culture

The LLC-PK$_1$ (pig kidney cells) cell line was purchased from the American Tissue Culture Company (ATCC). Cells were grown in Medium 199 with HEPES modification (Sigma) supplemented with 2.2 g L^{-1} NaHCO$_3$, 50 mg L^{-1} penicillin G, 50 mg L^{-1} streptomycin and 4% fetal calf serum (FCS). CCRF-CEM human lymphocytic leukemia cells were cultured in suspension (0.5 × 10^6 to 1.0 × 10^6 cells per mL) in RPMI 1640 medium (Sigma) supplemented with 10% FCS and the same antibiotics. The cells were incubated at 37 °C in the presence of 5% CO$_2$. Media for both cell lines was changed every 2–3 days until confluence or the maximum cell concentration was reached. Cells were subdivided

either by trypsin treatment (LLC-PK$_1$) to free cells from plates or after dilution in new media (CCRF-CEM).

Fluorescence spectroscopy of LLC-PK$_1$ cells

Cultured cells were grown in twenty 100 mm culture plates until confluence was attained. Culture media was discarded and the plates washed three times with cold cholate buffer, prepared by dissolving 2.47 g Na$_2$HPO$_4$, 0.53 g NaH$_2$PO$_4$, 17.0 g NaCl and 13.33 g choline chloride in 2 L MilliQ water. Cells were then gently scraped from the plates with a rubber cell scraper and pooled in Dulbecco's phosphate buffered saline (DPBS) (0.1 g L^{-1} MgCl$_2$·6H$_2$O, 0.2 g L^{-1} KCl, 0.2 g L^{-1} KH$_2$PO$_4$, 8.0 g L^{-1} NaCl, 1.15 g L^{-1} anhydrous Na$_2$HPO$_4$). Cells were collected by centrifugation at 680 g for 5 min and resuspended in 10 mL DPBS. The cell suspension was treated with 10 μM NPG$_E$ and incubated in the dark for one hour at 25 °C. For comparison, experiments were also conducted at 37 °C. To monitor the reaction between cells and NPG$_E$, a 1 mL aliquot (ca. 2.7 × 10^7 cells) was placed in a cuvette. Then, over a 40 min period and using an excitation wavelength of 505 nm, emission spectra were recorded between 515 nm and 600 nm with a Hitachi F-4500 fluorescence spectrophotometer. Afterwards, 10 μM N,N,N′,N′-tetrakis(2-pyridylmethyl)ethane-1,2-diamine (TPEN) was added and the fluorescence spectrum monitored for another 20 min. Finally, the reaction mixture was centrifuged using a microcentrifuge for about 5 min at 290 g to separate the extracellular medium and the cells, followed by resuspension of the cells in 1 mL DPBS.

Cell viability assay

Trypsinized 10^7 LLC-PK$_1$ cells were washed three times and resuspended in DPBS. Cells were then incubated with 10 μM NPG$_E$ for an hour at 25 °C. One hour later, 10^4 cells were reacted with 0.4% Trypan Blue solution in 1:1 ratio and viable cells were counted immediately using a hemocytometer. The cell viability assay was also used with culture medium.

Binding of NPG to cell constituents

After one hour incubation of cells with NPG$_E$ (see above), 9 mL of cell suspension were taken through the cycle of centrifugation and resuspension in fresh DPBS three times to remove extracellular NPG. The last cell pellet was resuspended in 1 mL of cold MilliQ water. Cells were then lysed by sonication and centrifuged at 47 000 g for 20 min at 4 °C to collect the cell supernatant. The supernatant was either loaded onto an 80 cm × 0.75 cm gel filtration column of Sephadex G-75 (GE Healthcare) equilibrated with 20 mM Tris buffer (pH 7.4) at room temperature or filtered through a Millipore Centricon Centrifuge filter (3 K M_W cut off) at 4 °C to separate the high and low molecular weight fractions. During gel-filtration chromatography, the column was eluted with degassed 20 mM Tris-Cl (pH 7.4) and ninety fractions were collected. Emission spectra of all fractions were obtained as described above. The zinc content in each fraction was also detected by flame atomic absorption spectroscopy (AAS).

Isolation of proteome using Sephadex G-75 chromatography

Cells were lysed by sonication and centrifuged at 47 000 g for 20 min to collect the cell supernatant, which was then loaded onto a Sephadex G-75 column as above. The supernatant was eluted with degassed 20 mM Tris-Cl (pH 7.4) and 1 mL fractions were collected. Fractions within the high molecular weight region having absorbance at 280 nm were pooled. These pooled fractions were referred to as the proteome. The protein concentration was measured using a BioRad DC Protein Assay kit; 2.0 mg mL^{-1} bovine serum albumin (BSA) served as the standard. Initially, 25 μL of sample was mixed with 125 μL alkaline copper tartrate and 1 mL dilute Folin reagent.[21,22] Then, 15 minutes later, the absorbance at 750 nm was recorded.

Isolation of subcellular proteomes

Subcellular proteomes were isolated as described with modifications.[23] LLC-PK$_1$ cells were collected and resuspended in 4 mL of pre-chilled homogenation buffer (0.25 M sucrose, 15 mM KCl, 1.5 mM MgSO$_4$, and 10 mM Tris-Cl pH 7.4). The cell suspension was then homogenized using a pestle and centrifuged at 1000 g for 10 min at 4 °C. The pellet was saved as the nominal membrane-nuclear fraction. Supernatant was then centrifuged at 10 000 g for 15 min at 4 °C. The pellet was retained as the mitochondrial fraction. Supernatant was centrifuged again at 100 000 g at 4 °C and the resultant supernatant was designated the cytosolic proteome. The membrane-nuclear and mitochondrial fractions were sonicated and centrifuged at 47 000 g for 20 min at 4 °C and the resultant supernatants were labelled as 'membrane/nuclear and mitochondrial proteomes, respectively.

Quantification of Zn^{2+} by atomic absorption spectrophotometry

The concentration of Zn^{2+} in solutions was determined by flame AAS. A GBC model 904 instrument employed an acetylene torch to atomize samples using an 80 : 20 mixture of compressed air and acetylene. Zinc measurements were made with deuterium background correction. The instrument was calibrated before each run using standard Zn^{2+} solutions.

Quantification of sulfhydryl groups

The concentration of sulfhydryl groups was determined with Ellman's Reagent.[24] Specifically, 60 μL of proteome sample was diluted with 540 μL 20 mM Tris-Cl, pH 7.4 and then incubated with 60 μL of 10 mM 5,5-dithiobis-2-nitrobenzoic acid (DTNB) for 30–60 min before the absorbance at 412 nm was obtained. An extinction coefficient of 13 600 cm^{-1} M^{-1} was used to determine the concentration of reactive thiol groups in the samples.

Results

Spectral properties of NPG and Zn–NPG

NPG$_E$ does not fluoresce but gains its fluorescent property upon conversion to NPG$_A$. With excitation at 505 nm, NPG$_A$ emitted fluorescence with a wavelength maximum at 530 nm. However, the fluorescence of NPG$_A$ and Zn–NPG$_A$ were not linearly dependent
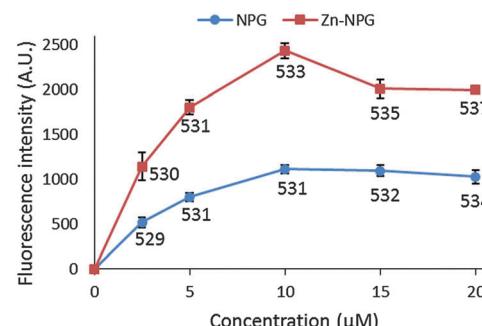

Fig. 2 Change of fluorescence intensity and emission wavelength maximum of NPG$_A$ and Zn–NPG$_A$ with increasing concentration. Equivalent amounts of NPG$_A$ and ZnCl$_2$ were mixed to make Zn–NPG complex. The numbers under each data point indicate the emission wavelength maximum of each spectrum in nanometers.

on their concentration (Fig. 2). With increasing concentration, their fluorescence intensity increased non-linearly until a maximum value after which it declined. Moreover, the emission wavelength maximum changed with concentration. The declining fluorescence intensity of NPG$_A$ and Zn–NPG$_A$ at higher concentration might be due to the stacking of fluorescein, the reporter part of NPG. This behavior rules out an inner filter effect as a possible reason. Regardless of the cause, this property of NPG$_A$ makes it difficult to quantify the actual Zn^{2+} concentration simply from the observation of fluorescence response. When titrated with Zn^{2+}, NPG$_A$ formed a 1 : 1 complex with its emission wavelength maximum unaltered and about twice the intensity of the free ligand (Fig. S1 and S2, ESI†). The product rapidly reacted with TPEN, a cell permeant, high affinity chelator of Zn^{2+}, returning the fluorescence to that of NPG$_A$ (Fig. S2, ESI†).

Cell viability

As the cellular experiments in this study were performed in DPBS buffer at 25 °C for an hour or so, the cell viability was determined under such conditions using Trypan Blue exclusion assay. Cell viability under experimental conditions was calculated to be 90%, whereas cells kept in culture medium were found to be almost 100% viable.

Reaction of NPG$_E$ with LLC-PK$_1$ cells

As a basis for addressing the question of what NPG images in cells, the reaction of NPG$_E$ with 10^7 LLC-PK$_1$ cells in DPBS buffer was monitored by spectrofluorimetry at 25° and 37 °C. At 25 °C, fluorescence intensity increased slowly at 530 nm, reaching a maximum after 40 min, indicative at least of the conversion of some NPG$_E$ to NPG$_A$ catalyzed by cellular esterases (Fig. 3A). The background fluorescence of media and cells was insignificant in comparison with the fluorescence contributed by the formation of NPG$_A$ (Fig. S3, ESI†). Considering the initial extracellular concentration of NPG$_E$, complete hydrolysis of the sensor would result in an intensity of about 5000 arbitrary units. Since the observed, maximal fluorescence was only about 1200 units, at most about 25% of NPG$_E$ had undergone reaction during this period. At that point, TPEN was added to quench


Proteome and low molecular weight fractions were assayed for Zn^{2+} and fluorescence. Zn^{2+} was associated with the high molecular weight proteome fractions, whereas fluorescent NPG$_A$ emerged from the column without bound Zn^{2+} well beyond the total volume of the column indicative of a favorable interaction between the Sephadex beads and NPG (Fig. S6, ESI†). Possibly, the chromatographic separation altered the original supernatant distribution. To investigate this possibility, proteome and low molecular weight species were separated using the Centricon filtration system and a 3 kDa cut-off filter. The majority of NPG$_A$ (about 85% of total fluorescence intensity) was retained by the filter during centrifugation along with the proteome (Fig. S7, ESI†). Thus, NPG$_A$ was weakly associated with protein in the supernatant but was dissociated from the proteome during Sephadex chromatography.

Reaction of NPG$_E$ with isolated proteome

In order to gain a more detailed understanding of the reaction of NPG with cells, an analogous set of experiments was conducted using isolated supernatant or proteome in place of whole cells. NPG$_E$ was slowly hydrolyzed to NPG$_A$ by supernatant or proteome, indicative of the presence of proteomic esterases that catalyze this conversion (Fig. 5). As in cells, much of the NPG$_A$ (84% of total fluorescence intensity) that was generated became associated with the proteome as shown by centrifugal filtration. The addition of TPEN failed to quench the proteome-associated fluorescence (Fig. S8, ESI†), consistent with the conclusion that NPG$_A$–Zn-proteins did not form during the enhancement of fluorescence.

Reactions of NPG with model Zn-proteins

The cellular and proteomic experiments with NPG indicate that the sensor does not successfully compete for native, proteomic Zn^{2+}. But they do not exclude the possibility that NPG may form ternary adducts with Zn-proteins that are insensitive to the presence of TPEN. To address this issue, NPG$_E$ was reacted with two model Zn-proteins, alcohol dehydrogenase (Zn-ADH) and

carbonic anhydrase (Zn-CA), that are known to form TPEN-sensitive ternary adducts with the Zn^{2+} sensors, TSQ and/or Zinquin.[5,16] Upon incubation of NPG$_E$ with Zn-ADH, the fluorescence gradually increased with time. However, TPEN was unable to quench the fluorescence. Therefore, the fluorescence increase was indicative of the capacity of ADH to act upon NPG$_E$ as an esterase not the ability of NPG to associate with one of ADH's bound Zn^{2+} ions. ZQ removes 1 Zn^{2+} from this protein as Zn(ZQ)$_2$ and binds to the other to form a fluorescent adduct.[5] Both are quenched by TPEN as it acquires Zn^{2+} from Zn(ZQ)$_2$ and displaces ZQ from ZQ–Zn-ADH to form TPEN–Zn-ADH.[5] Together with this information, the current result strongly implies that NPG neither binds to nor extracts Zn^{2+} from this protein. Similar results were obtained with Zn-CA; the protein has NPG$_E$ esterase activity but is otherwise unreactive with NPG. Nevertheless, the majority of NPG$_A$ did associate with Zn$_2$-ADH and Zn-CA according to Centricon filtration analysis.

Stability of Zn–NPG$_A$ with proteome

It was evident that NPG$_A$ cannot compete with native, protein bound Zn^{2+} to form Zn–NPG$_A$. We then inquired whether it can compete for adventitiously bound Zn^{2+} that might be produced under certain physiological or pathological conditions. Initially, 10 μM Zn–NPG$_A$ was titrated with proteome to test whether this species exhibits stability in the presence of protein competitors for Zn^{2+}. Fig. 6A shows that addition of proteome up to about 50 μg protein per mL (0–170 nM Zn^{2+} bound as Zn-protein) reduced the starting fluorescence intensity of Zn–NPG$_A$ to that of an equivalent concentration of NPG$_A$. Thus, NPG$_A$ does not compete favorably with proteome for Zn^{2+}.

The capability of NPG$_A$ to compete with proteome for Zn^{2+} was probed another way: 4.2 mg mL^{-1} proteome containing 7 μM Zn-proteins was mixed with 10 μM NPG$_A$ initially in 20 mM Tris (pH 7.4) and then titrated with Zn^{2+} (Fig. 6B). NPG$_A$ fluorescence did not increase until Zn^{2+} reached 30–35 μM or about 5× the total proteomic concentration of Zn^{2+}. At higher concentrations of Zn^{2+}, fluorescence emission at 535 nm increased; but even at 100 μM Zn^{2+}, stoichiometric Zn–NPG$_A$ had not been generated, showing that proteomic sites continued to partially sequester Zn^{2+} even at these large concentrations. Both experiments demonstrated that under the described conditions, NPG$_A$ has little, if any, capacity to compete with native proteome for Zn^{2+} that might be liberated from cellular binding sites during physiological or pathological processes.

We considered the possibility that proteins with substantial zinc buffering capacity might be distributed among some organelles and not able to interfere with NPG$_A$'s ability to image free or loosely bound Zn^{2+} in other compartments. To investigate this possibility, 1.7 mg mL^{-1} of cytosolic proteome (ca. 2.8 μM Zn^{2+}), isolated by gentle homogenization of cells followed by centrifugation at 100 000 × g, was mixed with 10 μM NPG$_A$ and subsequently titrated with Zn^{2+} (Fig. 6C). A detectable increase of fluorescence was not observed until the added Zn^{2+} reached about 10 μM. Beyond that, NPG$_A$ partially competed with cytosolic proteome for additional Zn^{2+}. This result was in
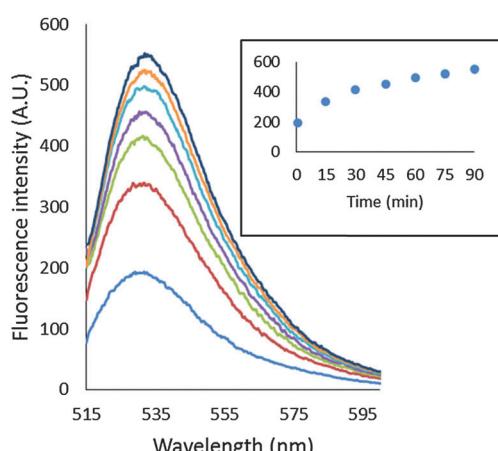
Fig. 5 Reaction of proteome with NPG$_E$. 4.2 mg mL^{-1} proteome containing 7 μM Zn^{2+} was incubated with 10 μM NPG$_E$ at ambient temperature (ca. 23 °C) for 90 min. The inset shows the progress of reaction with time.

A.
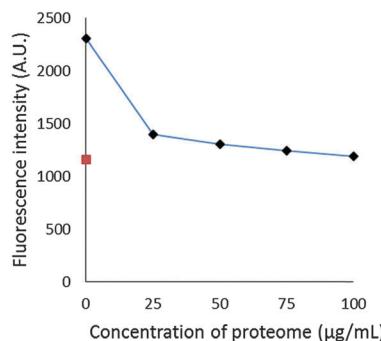
B.
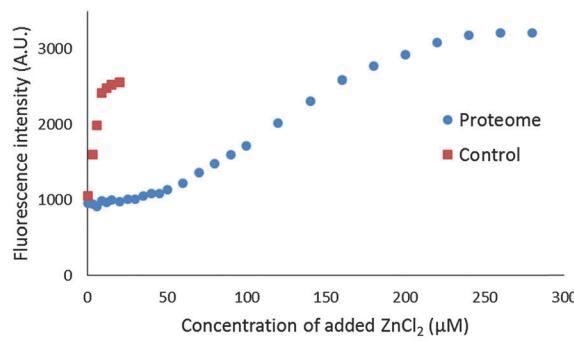
C.
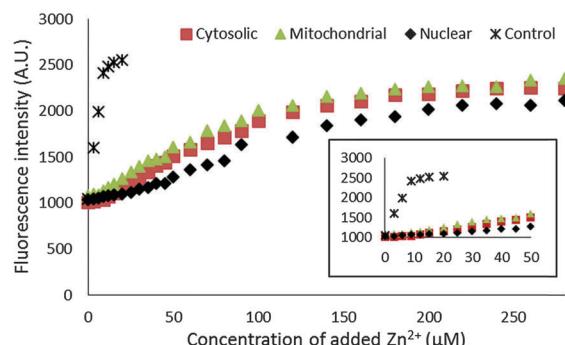

Fig. 6 Stability of Zn–NPG$_A$ with proteome. (A) Titration of 10 μM Zn–NPG$_A$ complex with proteome. The dilution of the sample by 100 μg mL^{-1} was only 2% and was ignored. The red square indicates the baseline fluorescence of 10 μM NPG$_A$. (B) Proteome: titration of 4.2 mg protein per mL (7 μM Zn^{2+} content) whole proteome with ZnCl$_2$ in the presence of 10 μM NPG$_A$. Control: titration of 10 μM NPG$_A$ with ZnCl$_2$. (C) Titration of 1.7 mg mL^{-1} cytosolic proteome, 1.6 mg mL^{-1} mitochondrial proteome and 1.6 mg mL^{-1} nuclear proteome with ZnCl$_2$ in the presence of 10 μM NPG$_A$. Initially, subcellular proteome was incubated with NPG$_A$ for 15 min. The incubation period of NPG$_A$ with the subcellular fractions after each addition of Zn^{2+} was 5 min. The inset highlights the initial buffering region.

qualitative agreement with the findings with whole proteome in the previous experiment and indicated that a subset of proteins within the cytosolic proteome possesses substantially higher affinity for free or loosely bound Zn^{2+} than does NPG$_A$. Similar results were obtained with membrane/nuclear and mitochondrial proteomes (Fig. 6C). All of the compartments displayed substantial Zn^{2+} buffering capacity.

A.
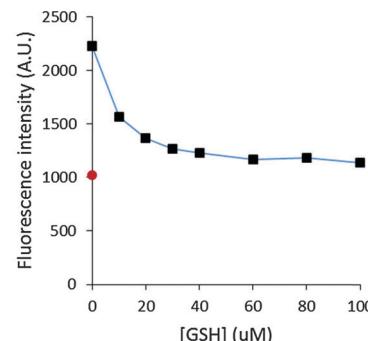
B.
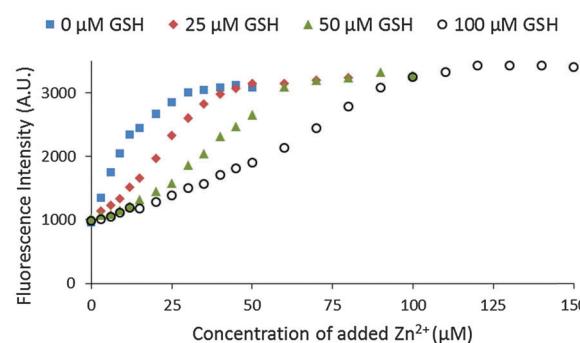
Fig. 7 Stability of Zn–NPG$_A$ with glutathione. (A) Titration of 10 μM Zn–NPG$_A$ complex with glutathione (GSH). The incubation period after each addition was 5 min. The dilution of the sample by 40 μM GSH was 2%. The red circle indicates the baseline fluorescence of 10 μM NPG$_A$. (B) Titration of 10 μM NPG$_A$ with ZnCl$_2$ in the absence or presence of various concentrations of glutathione. Initially, NPG$_A$ was mixed with GSH and for 5 min after each addition of Zn^{2+}.

Stability of Zn–NPG$_A$ with glutathione

The stability of Zn–NPG$_A$ was also studied in the presence of glutathione (GSH). GSH exists in the cells in mM concentration and displays modest affinity for Zn^{2+} ($10^{4.2}$ (Zn-SG) and $10^{5.7}$ (Zn(SG)$_2$) pH 7.2, 25 °C).[26] As little as 30 μM of GSH decreased the fluorescence intensity of 10 μM Zn–NPG$_A$ by almost 80% (Fig. 7A). The competition of glutathione for Zn^{2+} with NPG$_A$ was also confirmed by the titration of NPG$_A$ with Zn^{2+} in the presence of glutathione (Fig. 7B).

Response of intracellular NPG$_A$ to added Zn^{2+}

The stability of Zn–NPG$_A$ within the cellular environment was also investigated. To do so, 1.5×10^7 LLC-PK$_1$ cells were reacted with 10 μM NPG$_E$ for 30 min followed by washing to remove any remaining extracellular medium. The cells resuspended in DPBS were subsequently treated for 20 min with a pre-incubated mixture of 10 μM ZnCl$_2$ and 2 μM pyrithione, which served as an ionophore to conduct Zn^{2+} into cells. During this time the internal concentration of Zn^{2+} increased from 1.8 nmoles per 10^7 cells to 2.6 nmoles per 10^7 cells, representing 15% of the added Zn^{2+}. An increase of fluorescence (173% of control) was observed after the addition of Zn-pyrithione (Fig. 8). However, 10 μM EDTA rapidly reversed the fluorescence to 104% of control
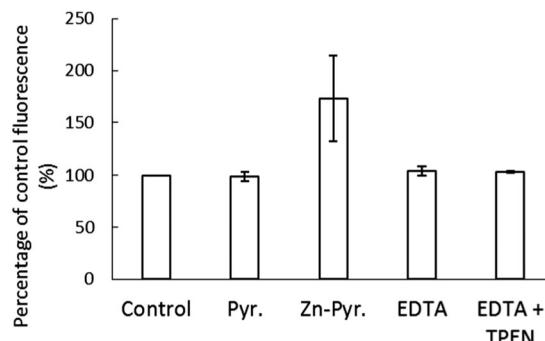
Fig. 8 Reaction of NPG$_E$ incubated LLC-PK$_1$ cells with Zn-pyrithione. 1.5 × 10^7 cells were treated with 10 μM NPG$_E$ for 30 min, washed twice and resuspended in DPBS (control). A pre-incubated mixture of 10 μM ZnCl$_2$ and 2 μM pyrithione was then added for 20 min. Pyr. indicates pyrithione. Subsequently, 10 μM EDTA was introduced for 10 min followed by 10 μM TPEN for another 10 min. Error bar represents standard error for three measurements.

suggesting that the elevation in fluorescence was mostly due to the binding of extracellular Zn^{2+} to NPG$_A$ that had diffused out of the cells. The inability of 10 μM TPEN to quench the remaining fluorescence ruled out the possibility that the residual 4% increase in fluorescence originated from binding of added Zn^{2+} to intracellular NPG$_A$. Instead, it probably arose from the continuing hydrolysis of intracellular non-fluorescent NPG$_E$ to fluorescent NPG$_A$. Thus, although the intracellular Zn^{2+} concentration had increased almost 50%, no Zn–NPG$_A$ was observed in the cells. Therefore, the results indicated that the intracellular NPG$_A$ did not compete for adventitious Zn^{2+} within the cellular environment.

Reaction of proteome with thiol reactive agents NO and NEM in the presence of NPG$_A$

To further examine if NPG$_A$ can image Zn^{2+} released from Zn-proteins, 3.6 mg mL^{-1} proteome containing 12 μM Zn-proteins was reacted with 200 μM of the nitric oxide donor, diethylamine NONOate (DEA-NO), in the presence of 10 μM NPG$_A$. The NO produced from the breakdown of DEA-NO can react with sulfhydryl groups in the Zn binding sites of the Zn-proteins resulting in the release of Zn^{2+}.[27] A 17% increase of fluorescence upon addition of DEA-NO was observed, which initially pointed to the release of Zn^{2+} and the subsequent formation of Zn–NPG$_A$ (Fig. 9A). However, the observation that TPEN did not reduce the fluorescence undermined this possibility. As a control, NPG$_A$ was reacted with DEA-NO to see if the sensor, itself, underwent reaction with DEA-NO. A 50% increase of fluorescence was observed upon its reaction with DEA-NO for 2 hours (Fig. 9A). Apparently, NPG$_A$ directly reacts with NO released from DEA-NO, resulting in an enhancement of fluorescence.

NPG$_A$'s weak ability to image adventitious Zn^{2+} released from the Zn-proteome was further verified with the use of another thiol binding reagent, N-ethylmaleimide (NEM). 5.14 mg mL^{-1} proteome containing 17 μM Zn-proteins was reacted with NEM. A total of 500 μM NEM reduced the
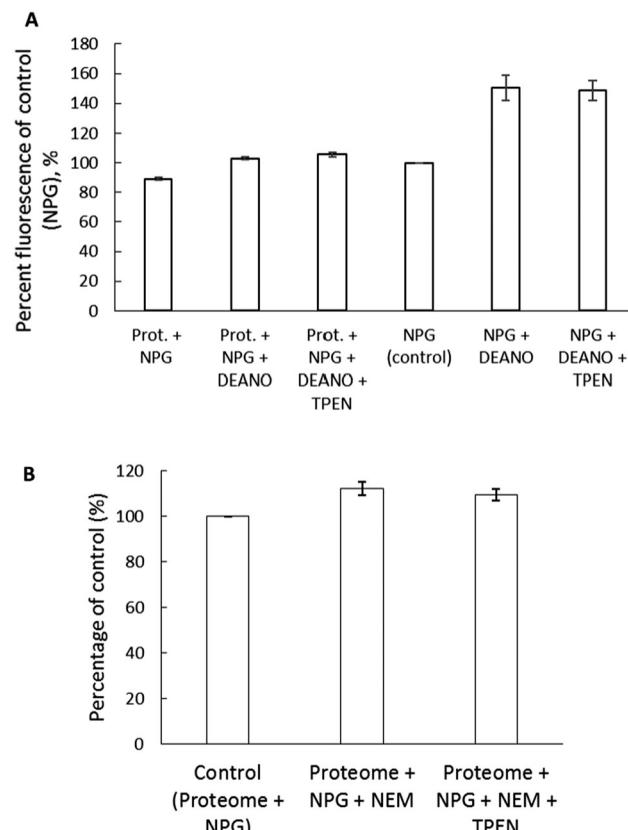
Fig. 9 Reaction of proteome with the thiol binding reagents. (A) Reaction of proteome (10 μM Zn^{2+}) with 200 μM DEA-NO for 90 min in the presence of 10 μM NPG$_A$ followed by the treatment with 10 μM TPEN for 30 min. The fluorescence was recorded continuously. 10 μM NPG$_A$ in Tris was reacted with 200 μM DEA-NO for 2 hours as a control. Prot. indicates proteome. (B) Reaction of proteome with 500 μM NEM in the presence of 10 μM NPG$_A$ for 30 min and the subsequent treatment with 30 μM TPEN for another 30 min. Error bar represents standard error for three measurements.

proteomic thiol concentration by almost 50% and caused about a 12% increase of fluorescence of 10 μM NPG$_A$, maximally equivalent to the formation of about 1 μM Zn–NPG$_A$ (Fig. 9B). The addition of 30 μM TPEN for 30 min reduced the fluorescence to 109% of control. Thus, no more than 0.3 μM Zn–NPG$_A$ had actually formed. In contrast, substituting 20 μM Zinquin for NPG$_A$, the higher affinity zinc sensor displayed a 47% increase of fluorescence after addition of only 100 μM NEM to the proteome. In the process, 25% of the proteomic zinc (4.2 μM) was labilized by NEM, much of it becoming bound to Zinquin.[20]

Discussion

NPG is a sensor that has been employed in a number of studies to image Zn^{2+}.[7–14] Within the general framework for understanding the behavior of metal sensors laid out in the Introduction, the use of NPG immediately raises questions. Its small stability constant for Zn^{2+} means that it has many potential competitors for available Zn^{2+} within the cell. Moreover, the

results of this study indicate that the use of NPG is complicated by several of its chemical properties.

In typical experiments, cells were initially incubated with NPG_E, a charge neutral form of the sensor employed to facilitate its uptake. Within cells NPG_E was converted to the negative charged NPG_A, which has been thought to undergo little or no efflux from cells. The conversion of NPG_E to NPG_A also transformed it into a molecule that emits fluorescence with a wavelength maximum of 530 nm (Fig. 3A). Trapped within cells, NPG_A is supposed to carry out its role of binding Zn^{2+} with a further enhancement in fluorescence.

The hydrolysis of NPG_E to NPG_A by esterases in LLC-PK$_1$ cells was slow (Fig. 3A). Thus, the kinetics of NPG_A formation may well overlap with putative reactions involving the mobilization of Zn^{2+} that are to be monitored by the formation of Zn–NPG_A. Moreover, according to *in vitro* titration results, NPG_A's Zn^{2+}-dependent enhancement of fluorescence only doubled the signal of NPG_A and did not change its emission spectrum. Thus, at best, Zn^{2+} binding is signaled by an increase in background fluorescence. Because of these characteristics, it is imperative to test for the formation of Zn–NPG_A by adding TPEN, a powerful, cell-permeant chelator of Zn^{2+} that readily and rapidly undergoes ligand substitution with Zn–NPG_A.[10,11] In LLC-PK$_1$ cells, the presence of TPEN did not alter the fluorescence emission of cells treated with NPG_E (Fig. 3A). Therefore, it was concluded that NPG_A did not compete effectively for Zn^{2+} in its native cellular distribution to form Zn–NPG_A.

In other studies, TPEN readily quenched the fluorescence acquired by cells exposed to TSQ or Zinquin.[5,20,25] Those sensors form ternary adducts with Zn-proteins as their mechanism of fluorescence enhancement. Detailed experiments showed that TPEN both obtained Zn^{2+} from Zn-proteins and replaced TSQ or ZQ in sensor-Zn-protein adducts as means to quench fluorescence.[25] On the basis of those reports, it was also concluded that the invariance of NPG_A-related fluorescence in the presence of TPEN indicated that NPG_A probably did not form adduct species with Zn-proteins. Similar results were seen in the reaction of NPG_E with Zn-alcohol dehydrogenase and Zn-carbonic anhydrase. The fluorescence increased as NPG_E was hydrolyzed to NPG_A by the enzymes, but the addition of TPEN failed to decrease the fluorescence intensity.

A peculiarity of the reaction of cells with NPG_E was that much of the NPG_A generated upon hydrolysis of NPG_E was found in the extracellular medium at either 25° or 37 °C. Data in Fig. 3B and 4 demonstrated that intracellular NPG underwent efflux either as NPG_E or NPG_A and appeared in the extracellular compartment as NPG_A. To the extent that such reactions occur, fluorescence enhancement attributable to the formation of Zn–NPG_A might involve Zn^{2+} outside the cell.

Features of the reaction of NPG_E with cellular components were explored further in experiments that incubated NPG_E and NPG_A with LLC-PK$_1$ cell proteome. As with intact cells, the proteome was able to hydrolyze NPG_E to NPG_A (Fig. 5). However, subsequent incubation with TPEN exerted no effect on the observed fluorescence, consistent with the conclusion that NPG_A neither formed Zn–NPG_A nor NPG_A–Zn-protein adducts

during the reaction. With both cells and proteome, the majority of NPG_A associated with the proteome possibly through interactions of the fluorescein ring with proteins. The interaction of NPG_A with proteins was further supported by its binding to the model proteins alcohol dehydrogenase and carbonic anhydrase. In both cases, most of the fluorescence was found associated with the protein though not with protein-bound Zn^{2+}. A recent paper also reported the association of NPG with proteomic fractions after gel filtration.[28]

The use of NPG as a Zn^{2+} sensor is rendered problematic by its small stability constant. Should a physiological or pathological process liberate Zn^{2+} in a concentration range (μM) that otherwise might make it accessible to reaction with NPG, numerous proteomic sites would also compete for binding.[15,29] Thus, according to the results shown in Fig. 6B, about 30–35 μM Zn^{2+} could be added to proteome containing 7 μM Zn^{2+} in the form of native Zn-proteins in the presence of 10 μM NPG_A before any Zn–NPG_A formed. Likewise, upon addition of 10 μM Zn–NPG_A to the same concentration of proteome as above, the fluorescence due to the Zn^{2+} complex was totally quenched as Zn^{2+} was transferred to the proteome (data not shown). According to the first experiment, Zn^{2+} at about 5× the total concentration of the Zn-proteome must be present before proteomic binding sites for adventitious Zn^{2+} are sufficiently titrated to permit the appearance of Zn–NPG_A. Similar zinc buffering capacity was obtained for the cytosolic, mitochondrial and nuclear proteomes (Fig. 6C).

Two experiments with thiol reactive reagents tested the primary hypothesis that NPG_A cannot compete with proteome for Zn^{2+} that is mobilized from Zn-proteome. After Zn-proteome was reacted with the NO donor, DEA-NO, NPG_A did not detect any accessible Zn^{2+} (Fig. 9A). It was apparent that components of the proteome bind the newly labilized Zn^{2+} with higher affinity than NPG_A, further deepening the question whether NPG can serve as a reliable intracellular sensor of Zn^{2+}.

A number of studies have employed NPG_A to image intracellular Zn^{2+} released through induction by NO and have reported fluorescence enhancement attributed to the formation of Zn–NPG_A.[30,31] Ironically, in the absence of Zn^{2+}, NPG_A images NO with an enhancement of fluorescence emission and an unchanged emission maximum (Fig. 9A). Taken together, the present findings encourage a re-examination of the studies that have detected Zn^{2+} released in cells by NO donors.

Results with another thiol binding reagent, NEM, also fail to support the imaging of Zn^{2+} liberated from Zn-proteome by NPG_A (Fig. 9B). Despite the reduction of sulfhydryl groups by 50% upon incubation of proteome with 500 μM NEM, only a non-significant enhancement of fluorescence intensity corresponding to about 0.3 μM Zn–NPG_A was sensitive to the presence of TPEN. By contrast, Zinquin, a sensor with higher stability constant for Zn^{2+}, binds proteomic Zn^{2+} mobilized by 100 μM NEM as $Zn(ZQ)_2$.[20] It appears that components of the proteome bind the newly labilized Zn^{2+} with higher affinity than NPG_A, further underscoring the problems with using NPG as an intracellular sensor of Zn^{2+}.

Besides proteome, the other major source of cellular metal binding sites is glutathione.[29,32] As with proteome, Zn–NPG_A

was unstable in the presence of GSH in the micromolar concentration range (Fig. 7). Since, glutathione exists in millimolar concentrations within cells, it is evident that GSH as well as proteome constitutes a powerful competitor of NPG_A for mobile Zn^{2+}.

In vivo findings were consistent with these *in vitro* results. Cells pre-incubated with NPG_E did respond to the addition of Zn^{2+} and the ionophore, pyrithione with a prompt increase in fluorescence (Fig. 8). However, most of the increase occurred in the extracellular medium where negatively charged EDTA competed with Zn–NPG_A and diminished the observed fluorescence. This result was suggestive of the conversion of NPG_E to NPG_A within the cells followed by its efflux in agreement with the results shown in Fig. 4. The fluorescence that remained from NPG_A within the cells was not impacted by the further addition of TPEN, even though pyrithione had shuttled in an amount of Zn^{2+} equal to 50% of the total proteomic concentration of Zn^{2+}. It was evident that intracellular Zn^{2+} competitors had successfully prevented the formation of Zn–NPG_A. Thus, it is unclear under what conditions NPG_A might be able to image intracellular Zn^{2+} that has been mobilized by some process. According to proteomic titrations of Zn^{2+} in Fig. 6, more than the total Zn^{2+} content of the entire proteome would be required to detect Zn–NPG_A. Possibly, much larger concentrations of intracellular NPG_A would need to be present than could be achieved in the current work in order to compete for Zn^{2+} in the presence of proteome and GSH.

Under some extreme conditions, such as at very large concentration of added Zn^{2+}, NPG_A can apparently form Zn^{2+}-NPG_A with an enhancement of fluorescence emission.[7,8,33–35] This may be expected either because extracellular Zn^{2+} is being imaged by NPG_A released from cells or because after the adventitious cellular binding sites for zinc are saturated with added Zn^{2+}, NPG_A binds excess Zn^{2+} with an accompanying increase in fluorescence intensity.

Other studies using NPG_A have reported stimulated Zn^{2+} release from different intracellular stores.[10,11,13] According to our study, in the presence of adventitious proteome binding sites and high concentration of glutathione, NPG_A is not likely to bind the released Zn^{2+} unless very large concentrations of extracellular Zn^{2+} are involved. Perhaps, the reported studies are dealing with the regions of the cells with low zinc buffering capacity or the experimental conditions induce the release of very large concentrations of Zn^{2+} that saturate the adventitious zinc binding sites before binding to NPG_A. However, our inquiry into subcellular Zn^{2+} buffering capacity did not find such organelle compartments (Fig. 6).

A possibility is to use NPG_A as an extracellular sensor of Zn^{2+} where Zn^{2+} buffering might be lower. Here, too, because of its modest stability constant for binding Zn^{2+}, the ability of NPG_A to serve as a sensor depends on the metal chelation capacity of the external medium. For example, if its composition were similar to that of plasma, a previous study of the reactivity of various Zn-bis-thiosemicarbazones with plasma demonstrated that Zn-complexes with apparent stability constants at pH 7 of 10^6 are not stable.[36]

Conclusion

A number of papers have reported positive results when using NPG as a Zn^{2+} sensor.[7–14] In contrast, the present work questions the stability of Zn–NPG_A in cell compartments. Because of its low stability constant for Zn^{2+}, NPG_A must compete with a host of adventitious proteomic sites possessing higher affinity for Zn^{2+}. Therefore, these results bring into question what pools of Zn^{2+} inside or outside cells and tissues may be imaged by NPG.

Acknowledgements

References

1 E. L. Que, D. W. Domaille and C. J. Chang, *Chem. Rev.*, 2008, **108**, 1517–1549.

2 M. D. Pluth, E. Tomat and S. Lippard, *Annu. Rev. Biochem.*, 2011, **80**, 333–355.

3 K. P. Carter, A. M. Young and A. E. Palmer, *Chem. Rev.*, 2014, **114**, 4564–4601.

4 D. H. Petering, *Chemtracts: Inorg. Chem.*, 2004, **17**, 569–580.

5 A. B. Nowakowski and D. H. Petering, *Inorg. Chem.*, 2011, **50**, 10124–10133.

6 R. P. Haugland, *Handbook of Fluorescent Probes and Research Products*, Molecular Probes, Inc., Eugene, OR, 9th edn, 2002.

7 L. M. Canzoniero, D. M. Turetsky and D. W. Choi, *J. Neurosci.*, 1999, **19**, RC31.

8 T. Priel, B. Aricha-Tamir and I. Sekler, *Eur. J. Pharmacol.*, 2007, **565**, 232–239.

9 C. J. Stork and Y. V. Li, *J. Neurosci. Methods*, 2006, **155**, 180–186.

10 S. Yamasaki, K. Sakata-Sogawa, A. Hasegawa, T. Suzuki, K. Kabu, E. Sato, K. Tomohiro, S. Yamashita, M. Tokunaga, K. Nishida and T. J. Hirano, *Chem. Biol.*, 2007, **177**, 637–645.

11 C. J. Stork and Y. V. Li, *J. Neurosci.*, 2006, **26**, 10430–10437.

12 B. Lukowiak, B. Vandewalle, R. Riachy, J. Kerr-Conte, V. Gmyr, S. Belaich, J. Lefebvre and F. Pattou, *J. Histochem. Cytochem.*, 2001, **49**, 519–527.

13 C. J. Stork and Y. V. Li, *J. Mol. Signaling*, 2010, **5**, 5.

14 E. Ohana, E. Hoch, C. Keaser, T. Kambe, O. Yifrach, M. Hershfinkel and I. Sekler, *J. Biol. Chem.*, 2009, **284**(26), 17677–17686.

15 A. Krezel and W. Maret, *JBIC, J. Biol. Inorg. Chem.*, 2006, **11**, 1049–1062.

16 D. J. Eide, *Biochim. Biophys. Acta*, 2006, **1763**, 711–722.

17 C. E. Outten and T. V. O'Halloran, *Science*, 2001, **292**, 2488–2492.

18 J. L. Vinkenborg, T. J. Nicolson, E. A. Bellomo, M. S. Koay, G. A. Rutter and M. Merkx, *Nat. Methods*, 2009, **6**, 737–740.

19 J. W. Meeusen, H. Tomasiewicz, A. Nowakowski and D. H. Petering, *Inorg. Chem.*, 2011, **50**(16), 7563–7573.

20 A. Nowakowski and D. Petering, *Metallomics*, 2012, **4**, 448–456.

21 O. H. Lowry, N. J. Rosebrough, A. L. Farr and R. J. Randall, *J. Biol. Chem.*, 1951, **193**, 265–275.

22 G. L. Peterson, *Anal. Biochem.*, 1979, **100**, 201–220.

23 D. H. Petering, J. Loftsgaarden, J. Schneider and B. Fowler, *Environ. Health Perspect.*, 1984, **54**, 73–81.

24 G. Ellman and H. Lysko, *Anal. Biochem.*, 1979, **93**, 98–102.

25 J. W. Meeusen, A. Nowakowski and D. H. Petering, *Inorg. Chem.*, 2012, **51**, 3625–3632.

26 M. J. Walsh and B. A. Ahner, *J. Inorg. Biochem.*, 2013, **128**, 112–123.

27 M. Malavolta, L. Costarelli, R. Giacconi, E. Muti, G. Bernardini, S. Tesei, C. Cipriano and E. Mocchegiani, *Cytometry, Part A*, 2006, **69**, 1043–1053.

28 J. A. Figueroa, K. S. Vignesh, G. S. Deepe Jr and J. Caruso, *Metallomics*, 2014, **6**, 301–315.

29 A. Nowakowski, M. Karim and D. H. Petering, Zinc proteomics, *Encyclopedia of Inorganic and Bioinorganic Chemistry*, 2015, pp. 1–10.

30 C. Kruczek, B. Gorg, V. Keitel, E. Pirev, K. D. Kroncke, F. Schliess and D. Haussinger, *Glia*, 2009, **57**, 79–92.

31 Y. Jang, H. Wang, J. Xi, R. A. Muller, E. A. Norfleet and Z. Xu, *Cardiovasc. Res.*, 2007, **75**, 426–433.

32 W. Maret, *Metallomics*, 2015, **7**, 202–211.

33 G. A. Kerchner, L. M. T. Canzoniero, S. P. Yu, C. Ling and D. W. Choi, *J. Physiol.*, 2000, **528**(1), 39–52.

34 G. Kovacs, N. Montalbetti, M. Franz, S. Graeter, A. Simonin and M. A. Hediger, *Cell Calcium*, 2013, **54**, 276–286.

35 S. L. Sensi, H. Z. Yin, S. G. Carriedo, S. S. Rao and J. H. Weiss, *Proc. Natl. Acad. Sci. U. S. A.*, 1999, **96**, 2414–2419.

36 D. H. Petering, *Biochem. Pharmacol.*, 1974, **23**(3), 567–576.